ARTICLES

Double-Layered TiO_2−SiO_2 Nanostructured Films with Self-Cleaning and Antireflective Properties†

Xintong Zhang, Akira Fujishima,* Ming Jin, Alexei V. Emeline, and Taketoshi Murakami

Special Laboratory for Optical Sciences, Kanagawa Academy of Science and Technology, 3-2-1 Sakado, Takatsu-ku, Kawasaki-shi, Kanagawa 213-0012, Japan

Received: July 13, 2006; In Final Form: September 22, 2006

Dual functions of self-cleaning and antireflection can be created in double-layered TiO_2−SiO_2 nanostructured films. The films were prepared by (1) layer-by-layer deposition of multilayered SiO_2 nanoparticles with polydiallyldimethylammonium (PDDA) cations, (2) layer-by-layer deposition of multilayered titanate nanosheets with polycations on PDDA/SiO_2 multilayer films, and (3) burning out the polymer and converting titanate nanosheets into TiO_2 by heating at 500 °C. The as-prepared films, consisting of a porous SiO_2 bottom layer and a dense TiO_2 top layer, improved the transmittance of glass or quartz substrates, as demonstrated by transmission spectra collected at normal incidence. The photocatalytic properties of the films were studied by the change of the water contact angle together with the decay of the IR absorption of the hydrocarbon chain of octadecylphosphonic-acid-modified films under 2.6 mW cm^{-2} UV illumination. Both the antireflective and the photocatalytic properties of the films were dependent on the number of PDDA/nanosheet bilayers deposited. However, excellent surface wettability of the films for water was obtained, independent of the preparation conditions. The experimental findings are discussed in terms of the special structure of the double-layered nanostructured film.

Introduction

Since the discovery of photostimulated water splitting on TiO_2 electrodes by Fujishima and Honda three decades ago,[1] extensive research has been carried out on TiO_2 for the purpose of solar energy conversion [2−4] and environmental cleanup.[5−9] Among a myriad of applications of TiO_2, the self-cleaning surface, which utilizes sunlight and natural rainfall to keep the surface clean, is one of the most interesting and attractive, since it can save a lot of time, cost, and energy for maintenance.[8−10] TiO_2, excited by the UV light in solar illumination, can decompose oily contaminants adhering to the surface.[11−15] The superhydrophilic property of TiO_2 stimulated by UV light facilitates the spread and flow of water droplets on the surface, which also aids the decontamination process.[16,17] Various self-cleaning products, such as tiles, glass, and plastics, etc., have become commercially available and have exhibited dependable quality.[10]

TiO_2 has a large refractive index ($n \approx 2.52$ for anatase) and thus can reflect a large portion of incident light.[18] When it is applied on transparent materials to provide a self-cleaning function, careful control of the film composition is often needed to suppress surface reflection. A general method is to prepare a composite of TiO_2 with SiO_2, a material of low refractive index, so as to reduce the refractive index of the film close to transparent substrates.[10] However, this method is not appropriate for possible self-cleaning applications in solar cells, solar heating devices, and green houses, etc., where low surface reflection, i.e., high light transmittance, are favored.[19,20]

To obtain low surface reflection, one may make the refractive index of the film lower than that of the substrate materials through an increase of the porosity.[21−24] This idea has been examined in our previous work, in which a sub-monolayer of SiO_2 particles (∼100 nm) was covered with TiO_2 nanoparticles to generate a low-refractive-index film and maintain the self-cleaning properties at the same time.[25] However, due to the large refractive index of TiO_2, the volume percentage of TiO_2 should be very low (∼5%) to create effective antireflection, which is undesirable for the self-cleaning function. In the present work, we examined the possibility of creating the dual functions of self-cleaning and antireflection in double-layered TiO_2−SiO_2 films that consisted of dense top layer of TiO_2 and porous bottom layer of SiO_2. The films were prepared by layer-by-layer assembly of SiO_2 nanoparticles and titanate nanosheets with polycations, as summarized in Scheme 1. Titanate nanosheets, which have an extremely small thickness of 0.7 nm and lateral sizes ranging from less than a micrometer to several tens of micrometers,[26,27] were employed to form TiO_2 layers with precisely controllable thicknesses. This material was reported to undergo a phase transition to anatase-type TiO_2 in calcination.[28−30] The layer-by-layer assembly of SiO_2 nanoparticles[31−34] and nanosheets[29,35,36] has been well-studied; the present study emphasizes the creation of novel functions through the coassembly of both materials.

† Part of the special issue "Arthur J. Nozik Festschrift".

* Author to whom correspondence should be addressed. Phone: +81-44-819-2020. Fax: +81-44-819-2038. E-mail: Fujishima@newkast.or.jp.

10.1021/jp064442u CCC: $33.50
Published on Web 10/26/2006

SCHEME 1: Flow Chart for the Preparation of Double-Layered TiO_2-SiO_2 Self-Cleaning Coatings with Antireflective Properties

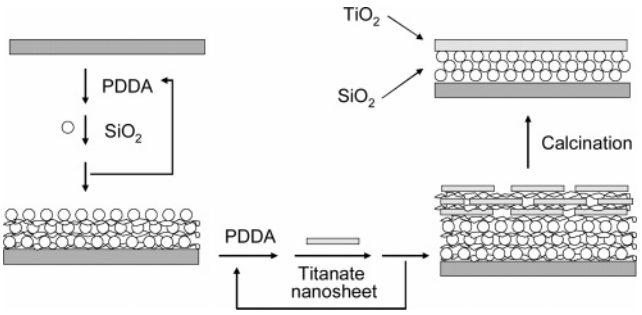

Experimental Section

Materials. Poly(diallyldimethylammonium) (PDDA, Aldrich, medium molecular weight), a linear quaternary ammonium polycation, was available commercially and was used without further purification at a concentration of 2 mg mL^{-1}. Aqueous SiO_2 colloidal solution (Cataloid SI-40, pH 8.8, 40.4 wt %), purchased from Catalyst Chemical Co., was diluted to a concentration of 1 mg mL^{-1} with deionized water. The colloidal solution contained spherical SiO_2 nanoparticles with an average diameter of 17 nm. Both PDDA and SiO_2 solutions were adjusted to pH ~9.0 with 0.1 mol L^{-1} aqueous ammonium solution, as in our previous work.[25] The pH condition was found to be important to prepare a stable SiO_2 colloidal solution. Titanate nanosheets of the composition $Ti_{1-\delta}O_2^{4\delta-}$ ($\delta \approx 0.09$) were synthesized by delaminating a layered protonic titanate compound of $H_{0.7}Ti_{1.825}\square_{0.175}O_4$ (where $\square$ represents a vacancy) in tetrabutylammonium (TBA) hydroxide solution according to the procedures of Sasaki.[37,38] The resultant suspension after delamination contains individual $Ti_{1-\delta}O_2^{4\delta-}$ ($\delta \approx 0.09$) nanosheets surrounded by TBA^+ cations. Before assembly, the nanosheet solution was diluted to a concentration of 0.08 g L^{-1}, and its pH value was carefully adjusted to 9.0 with 5 mmol L^{-1} tetrabutylammonium hydroxide solution.[29,34,35] Deionized water with a specific resistance of approximately 18 MΩ cm was used in all experiments. Octadodecyl phosphate was purchased from Wako Chemicals. Sovlents, such as heptane and 2-propanol, were purchased from Wako chemicals and were used without purification.

Preparation of Double-Layered Film. Glass and quartz substrates were cleaned with a concentrated H_2SO_4/H_2O_2 (7:3 v/v) solution and then washed with deionized water. (**Caution**: The H_2SO_4/H_2O_2 solution is highly dangerous and must be used with great care.) The washed substrates were alternatively dipped in PDDA and SiO_2 colloidal solutions for 5 min, with intermediate water washing. The deposition of the PDDA/SiO_2 bilayer was repeated six times so as to prepare multilayer films of $(PDDA/SiO_2)_6$. In the subsequent step, the $(PDDA/SiO_2)_6$ multilayer was alternatively dipped in PDDA and titanate nanosheet solutions for several cycles by the same procedures described above. Finally, the multilayer assemblies of SiO_2 nanoparticles and titanate nanosheets were converted to double-layered TiO_2-SiO_2 films by calcination at 500 °C for 1 h. This heating procedure burned out the polymer and caused a phase transition of the titanate nanosheets into anatase TiO_2.[28−30] Pure TiO_2 or SiO_2 films also were prepared by the same procedures and used in some experiments as reference samples.

Self-Cleaning Experiment. Double-layered TiO_2-SiO_2 films were modified with a monolayer of octadodecyl phosphate (ODP) by the reported method with a little modification.[39] Typically, the coated glass substrates were dipped into a 0.5 mmol L^{-1} solution of ODP in a mixed solvent of heptane and 2-propanol (1000:7 v/v). After being dipped over 48 h, the substrates were removed from the ODP solution and washed with 2-propanol. The films became hydrophobic after ODP treatment. To evaluate the self-cleaning properties, ODP-modified films were placed under a Hayashi LA-310 light source, which emits ultraviolet light in the range of 300−400 nm. Then, the photocatalytic decomposition of ODP on TiO_2-SiO_2 films was studied by measuring the water contact angle at 10 different positions on the films or by the decay of the symmetric and asymmetric vibrations of the $-CH_2-$ and CH_3- groups at intervals during UV illumination. The intensity of the light illuminated on the surface was maintained at 2.6 mW cm^{-2} in all experiments, as measured with a UV power meter (Hamamatsu Photonics, C9536-01).

Instrumentation. UV−vis transmission and absorption spectra of the films were measured with a Shimadzu UV-2450 spectrophotometer at normal incidence. Surface and cross-sectional morphologies of the films were examined with a Hitachi S-4500 scanning electron microscope. All of the samples were coated with platinum with a commercial sputtering apparatus prior to the scanning electron microscopy (SEM) measurements. The contact angle was measured with a contact angle meter (Kyowa CA-X) in the sessile mode at room temperature and analyzed with commercial FAMAS software. IR spectra were measured in transmission mode with a JASCO Fourier transform IR 6100 spectrometer (resolution 2 cm^{-1}). The refractive indices of the SiO_2 and TiO_2 films were measured with an ellipsometer (J. A. Woollam, M-2000U) in the wavelength region of 250−1000 nm.

Results and Discussion

Multilayer Assembly. Double-layered TiO_2-SiO_2 nanostructured films can be readily prepared by the procedures shown in Scheme 1. The bottom SiO_2 layer, stacked from spherical SiO_2 particles, is porous, while the top TiO_2 layer, made from unilamellar nanosheets, can be a dense layer. The porous SiO_2 layer, which exhibits a low refractive index,[33,34] can be antireflective as reported by Cebeci et al.[34] The TiO_2 top layer should provide photocatalytic and photoinduced superhydrophilic functions under UV illumination.[8−10] We expected the double-layered film to exhibit dual functions of self-cleaning and antireflection. To realize it, however, effort should be devoted to optimizing several film parameters, such as the thickness of each layer and the porosity of the SiO_2 layer. Since there have been several papers discussing the layer-by-layer assembly of SiO_2 nanoparticles,[25,31−34] we thus focused more attention here on the layer-by-layer assembly of nanosheets on the SiO_2 multilayer films. Cleaned quartz or glass substrates were first coated with six bilayers of PDDA/SiO_2 by alternating deposition. After this procedure, the surface reflection of the substrates became very weak and showed maximum transmittance (over 99.2% around 290 nm) that was greater than the 92.5% transmittance of bare quartz substrates at the same wavelength (Figure 1). A similar antireflective phenomenon was observed by Cebeci et al. on a poly(allylamine hydrochloride)/SiO_2 multilayer assembly, in which they explained the phenomenon by the low refractive index the of multilayers, a direct consequence of the porosity introduced by the random packing of SiO_2 nanoparticles.[34] Rouse et al. reported the extremely low refractive index of the PDDA/SiO_2 multilayer assembly, but they did not discuss the antireflective properties of their samples.[33] Increasing the number of PDDA/SiO_2 bilayers caused

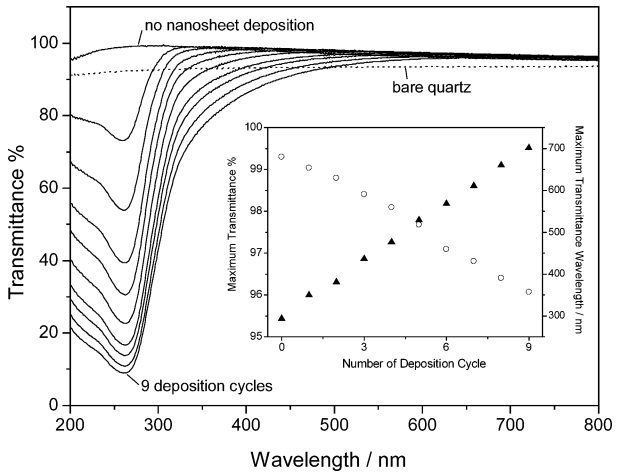

Figure 1. UV−vis transmittance spectra recorded during layer-by-layer deposition of nanosheets on a $(PDDA/SiO_2)_6$ multilayer film. Note that the substrates were coated on both sides with the multilayered film. Inset: Maximum transmittance (circle) and the most transmissive wavelength (triangle) of the multilayer assembly as a function of the nanosheet deposition cycle.

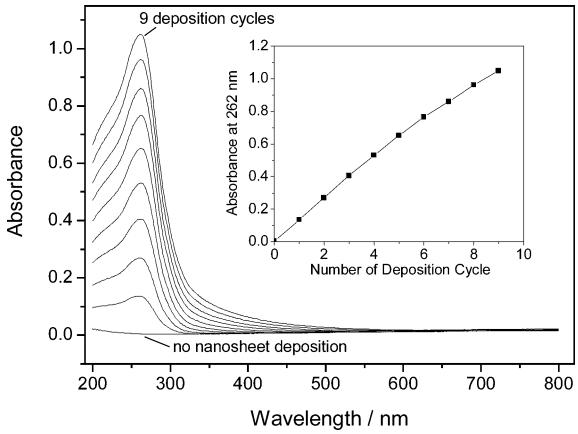

Figure 2. UV−vis absorption spectra recorded during layer-by-layer deposition of titanate nanosheets on a $(PDDA/SiO_2)_6$ multilayer film. The peak at 260 nm is characteristic of titanate nanosheets. Inset: Absorbance of multilayer film at 260 nm as a function of the nanosheet deposition cycle.

a red shift of the most transmissive wavelength, but the maximum transmittance did not change markedly. Hence, in the next experiments, if not specifically mentioned, we used $(PDDA/SiO_2)_6$ multilayer films as base materials to assemble the titanate nanosheets.

The assembly process of nanosheet multilayers was monitored with UV−vis spectra recorded after each deposition cycle, as depicted in Figures 1 and 2. The band appearing at approximately 262 nm is characteristic of titanate nanosheets.[29,35] PDDA, however, does not have an absorption in this spectral range. The peak increased nearly linearly (Figure 2, inset), indicating the regular growth of bilayers of PDDA/nanosheets on the $(PDDA/SiO_2)_6$ multilayers. The deposition of PDDA/nanosheet bilayers gradually lowered the light transmittance and shifted the most transmissive wavelength to the visible light region. This may be explained by the large refractive index of the nanosheets and the increase in film thickness. The decrease in light transmittance and the red shift of the most transmissive wavelength showed a nearly linear dependence on the number of PDDA/nanosheet bilayers (Figure 1, inset). After deposition of nine bilayers of nanosheets, the most transmissive wavelength was shifted to 700 nm, and the film lost its antireflective property at wavelengths shorter than 500 nm. When 12 bilayers were deposited, no antireflective property could be observed in the spectrum of visible light (400−800 nm).

Calcination of Multilayer Films. Titanate nanosheets are built up from edge-shared TiO_6 octahedra that are arrayed in a zigzag way to produce a two-dimensional sheet structure.[26,36] Approximately 9% of the octahedral site is not occupied by Ti atoms, yielding the negative charges.[26,36] Heating titanate nanosheet multilayers over 500 °C can cause the phase transition to anatase-type TiO_2 with high crystallinity, as reported by Sasaki et al.[28−30] This phase transition was also confirmed in our X-ray diffraction experiments (Supporting Information). Heating the multilayer assemblies of SiO_2 nanoparticles and titanate nanosheets at 500 °C led to the formation of double-layered TiO_2-SiO_2 films. SiO_2 films prepared from six bilayers of $PDDA/SiO_2$ were highly porous due to random packing of SiO_2 nanoparticles (Figures 3a and 3e). The large porosity resulted in a very low refractive index (1.27 at 633 nm) and thus is able to create antireflective properties. Deposition of PDDA/nanosheet bilayers on the $PDDA/SiO_2$ multilayers caused the formation of a double-layered structure after calcination, such that the porous layers of SiO_2 were covered with ultrathin dense layers of TiO_2 (Figures 3b−d). The dense layers followed the curvature of the surface of the porous SiO_2 layer (Figure 3f), with coverage closely related to the number of PDDA/nanosheet bilayers deposited. The dense TiO_2 layer prepared from three bilayers of PDDA/nanosheets resulted in a coverage of >80%. However, when the number of bilayers was increased to nine, nearly all of the SiO_2 layer was able to be covered with a dense TiO_2 layer, resulting in an interesting structure possibly holding the dual functions of self-cleaning and antireflection.

Figure 4 depicts the absorption spectra of the three double-layered films prepared from $(PDDA/SiO_2)_6/(PDDA/nanosheet)_x$ ($x = 3, 6, 9$). As a reference, the spectrum of the nanosheet colloidal solution is also shown in the figure. All of the films showed red-shifted absorption characteristics compared to that of the colloidal solution, also indicating a phase transition from titanate to TiO_2.[28−30] The band gap values (E_g) of the three films were estimated to be 3.65, 3.40, and 3.26 eV for x values of 3, 6, and 9, respectively, by eq 1, which gives the relationship between the absorption coefficient (α) and the energy of the exciting photons ($h\nu$) for an indirect semiconductor[2]

$$\alpha h\nu = \text{constant}(h\nu - E_g)^2 \qquad (1)$$

These band gap values are larger than the 3.2 eV band gap of bulk anatase because of the ultrathin nature of the TiO_2 layers. The thicknesses of the ultrathin TiO_2 layers measured by ellipsometry were 2.2, 4.3, and 6.5 nm for x values of 3, 6, and 9, respectively.[40] These data are consistent with the reported thickness of 0.72 nm for a single titanate nanosheet. The TiO_2 layers are so thin that they should exhibit a quantum confinement effect, i.e., a larger band gap value than that of bulk TiO_2.[41]

Antireflective Properties. Figure 5 depicts the transmission spectra of TiO_2-SiO_2 films prepared from $(PDDA/SiO_2)_6/(PDDA/nanosheet)_x$ ($x = 3, 6, 9$) multilayer assemblies. As references, the spectra of bare quartz and SiO_2 film prepared from $(PDDA/SiO_2)_6$ are also shown in the figure. Double-layered films all enhanced the transmittance of quartz substrates in the visible spectrum (400−800 nm), indicating their antireflective properties. In comparison to pure SiO_2 film, TiO_2-SiO_2 double-layered films exhibited a smaller maximum transmittance and red shifts of the most transmissive wavelength. The decrease

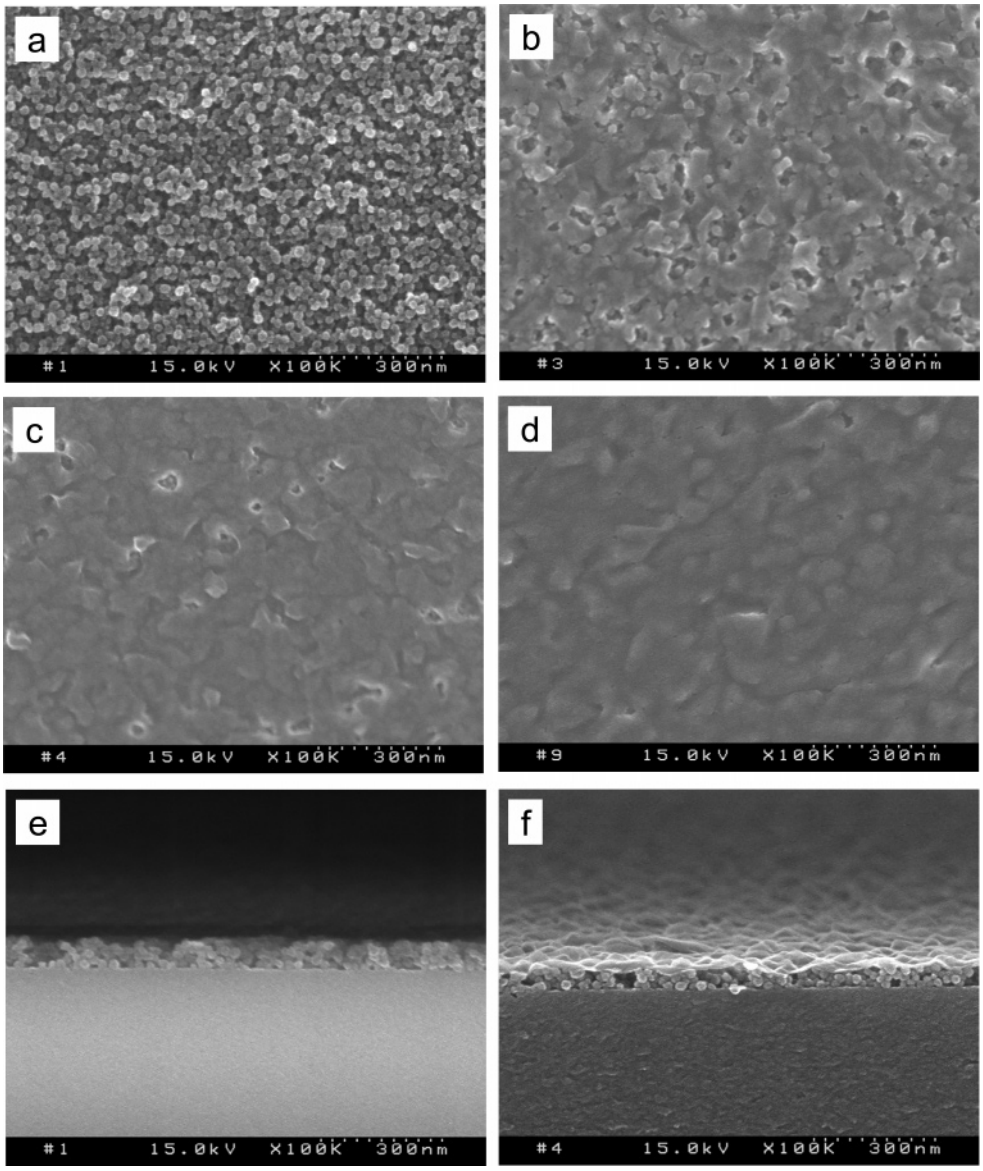

Figure 3. (a−d) Top-view scanning electron micrographs of $(PDDA/SiO_2)_6/(PDDA/nanosheet)_x$ multilayer films after calcinations at 500 °C: (a) $x = 0$; (b) $x = 3$; (c) $x = 6$; (d) $x = 9$. (e−f) Cross-sectional electron micrographs of $(PDDA/SiO_2)_6$ and $(PDDA/SiO_2)_6/(PDDA/nanosheet)_6$ multilayer films after calcination at 500 °C, respectively.

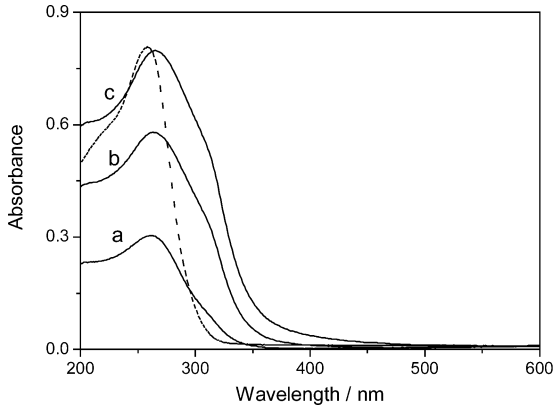

Figure 4. UV−vis absorption spectra of three TiO_2-SiO_2 double-layered films prepared from heating $(PDDA/SiO_2)_6/(PDDA/nanosheet)_x$ multilayer films: (a) $x = 3$; (b) $x = 6$; (c) $x = 9$. The absorption spectrum of the titanate nanosheet colloidal solution is shown in the figure as the dotted line.

in maximum transmittance as well as the red shift of the most transmissive wavelength of the double-layered films are both related to the number of PDDA/nanosheet bilayers (Figure 5, inset), when the characteristics of the SiO_2 layer were held constant, due to the large refractive index of TiO_2 and the increase in film thickness. One interesting finding was that the TiO_2 layer influenced the most transmissive wavelength greater than the SiO_2 layer. Six ultrathin bilayers of PDDA/nanosheet shifted the most transmissive wavelength of the SiO_2 layer by approximately 120 nm after heating. However, it required four bilayers of relatively thick $PDDA/SiO_2$ to accomplish a similar shift. Note that the thickness of the nanosheets is only 0.72 nm,[26,27] while the average size of the SiO_2 nanoparticles is approximately 17 nm.

Both the SiO_2 and the double-layered TiO_2-SiO_2 films exhibited greater transmittance and shorter maximum transmissive wavelengths than the multilayer films before heating. Burning out the high-refractive-index polymer (ca. 1.7),[29,34] which resulted in the lowering of the refractive index and the thinning of the films, should be the cause. The refractive indices of ultrathin TiO_2 films at 633 nm were 1.80, 2.04, and 2.07, respectively, for the 2.2-, 4.3-, and 6.5-nm-thick films. These values are smaller than the refractive index of 2.52 for bulk

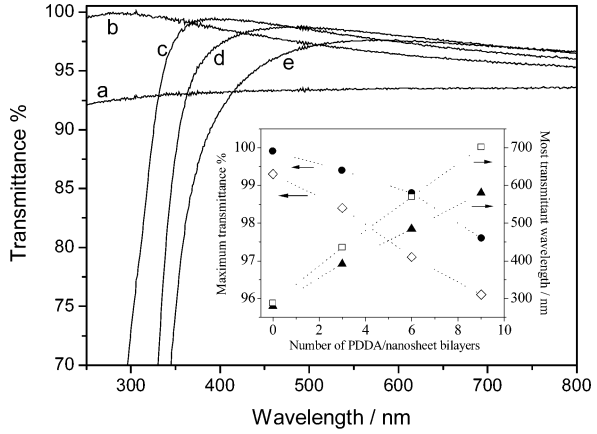

Figure 5. Transmission spectra of quartz substrates covered with double-layered TiO_2-SiO_2 films on both sides. The films were prepared by calcinations of $(PDDA/SiO_2)_6/(PDDA/nanosheet)_x$ multilayer films: (c) $x = 3$; (d) $x = 6$; (e) $x = 9$. For reference, transmission spectra of bare quartz and SiO_2 film prepared by calcinations of $(PDDA/SiO_2)_6$ multilayer film are shown as curves a and curve b, respectively. Inset: Maximum transmittance of $(PDDA/SiO_2)_6/(PDDA/nanosheet)_x$ multilayer film series before (diamonds) and after (circles) 500 °C calcination and the most transmissive wavelength of the same multilayer film series before (squares) and after (triangles) 500 °C calcination.

SCHEME 2: Double-Layered Antireflective Coating Showing the Various Parameters Used in the Text

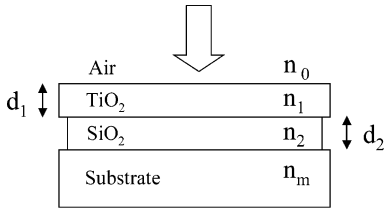

anatase, possibly due to their ultrathin structure, but are much greater than that of glass (refractive index: 1.52) or quartz (refractive index 1.46). Therefore, these ultrathin TiO_2 films always enhance the surface reflection of glass or quartz substrates if coated directly. Our studies, however, showed that the double-layered TiO_2-SiO_2 film could be antireflective for the above substrates in the whole visible spectrum, despite the large refractive index of the ultrathin TiO_2 layer. The key point should be the use of the porous SiO_2 layer of low refractive index (1.27 at 633 nm) as an interlayer.

We calculated the transmission spectrum at the normal incidence of a double-layered TiO_2-SiO_2 film by means of characteristic matrix theory.[42] The characteristic matrix for the film−substrate assembly shown in Scheme 2 is given by eq 2

$$\begin{pmatrix} B \\ C \end{pmatrix} = \begin{pmatrix} \cos\delta_1 & (i\sin\delta_1)/n_1 \\ in_1\sin\delta_1 & \cos\delta_1 \end{pmatrix} \times \begin{pmatrix} \cos\delta_2 & (i\sin\delta_2)/n_2 \\ in_2\sin\delta_2 & \cos\delta_2 \end{pmatrix} \begin{bmatrix} 1 \\ n_m \end{bmatrix} \quad (2)$$

where the phase thickness δ_i is related to the physical thickness d_i of the material by the expression $\delta_i = (2\pi/\lambda)n_i d_i$ for the normal incidence, $i = 1$ and 2. The admittance of the film−substrate assembly, Y, is given by eq 3

$$Y = \frac{C}{B} = [(n_m\cos\delta_1\cos\delta_2 - n_1 n_m\sin\delta_1\sin\delta_2/n_2) + i(n_1\sin\delta_1\cos\delta_2 + n_2\cos\delta_1\sin\delta_2)]/[(\cos\delta_1\cos\delta_2 - n_2\sin\delta_1\sin\delta_2/n_1) + i(n_m\sin\delta_1\cos\delta_2/n_2 + n_m\cos\delta_1\sin\delta_2/n_1)] \quad (3)$$

Then, the reflection at the film surface can be calculated from Y by eq 4

$$R = \left(\frac{n_0 - Y}{n_0 + Y}\right)\left(\frac{n_0 - Y}{n_0 + Y}\right)^* \quad (4)$$

and the transmission (T) at normal incidence can be calculated from the reflection (R), provided that no light absorption or scattering occur

$$T = 1 - R \quad (5)$$

We assumed a 6.5 nm thickness for the TiO_2 layer and a 55 nm thickness for the SiO_2 layer and input into eqs 2 and 3 the refractive index data for the SiO_2 and TiO_2 layers. Note that the thickness and refractive index were all obtained by ellipsometric measurements on SiO_2 films and TiO_2 ultrathin films, respectively.[43] We were thus able to calculate a transmission spectrum and compare it with the actual spectrum in Figure 6. The two spectra fit quite well, considering the errors in setting film parameters and the possible light scattering of the actual sample. Varying the thickness setting produced some interesting results. One of the results was that the maximum transmittance of the double-layered structure is determined by the thickness of the SiO_2 layer. The thicker the SiO_2, the greater the calculated transmittance. This result clearly explains the function of the porous SiO_2 layer in the double-layered film and should be valuable for optimizing the design of double-layered self-cleaning antireflective films.

Photocatalytic and Superhydrophilic Properties. The soiling of surfaces exposed outdoors is closely related to the contamination of oily organic substances on the surface to which airborne dust adheres. The TiO_2 surface can decompose organic contamination under sunlight; the adhering dust thus will be washed off easily by rainwater. In the present study, ODP was employed to simulate oily substances in the ambient environment that often have long hydrocarbon chains. This molecule can form a compact self-assembled monolayer on the surface of TiO_2 and result in a hydrophobic surface (contact angle over 100°).[44] Thus, we were able to monitor the photocatalytic decomposition of the ODP monolayer by means of contact angle measurements. UV light with a power of 2.6 mW cm^{-2} was used in this experiment, resembling the UV intensity of sunlight. TiO_2-SiO_2 double-layered films modified with an ODP monolayer showed significant decreases in water contact angle as a function of illumination time (Figure 7). Likewise, there were decreases in the amounts of $-CH_2-$ and CH_3- groups as measured by IR spectra (Figure 8). The simultaneous decreases in contact angle and IR signals for the hydrocarbon chain (2800−3000 cm^{-1}) provide clear evidence for the photocatalytic decomposition of ODP with double-layered TiO_2-SiO_2 films. The rates of contact angle decrease were dependent on the thickness of the TiO_2 layers. The thicker the TiO_2 layer, the faster the decrease of the water contact angle. This can be explained by the ability of the TiO_2 layer to absorb UV light, which is determined by the film thickness and absorption onset.

As the most important photocatalytic material, TiO_2 has strong oxidative power, with which it can completely decompose

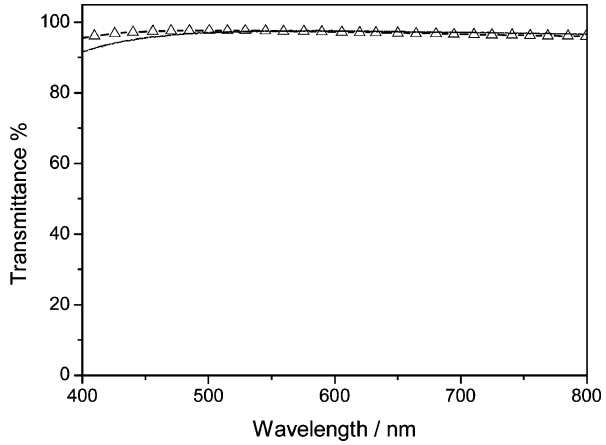

Figure 6. Calculated (triangles) and measured (dotted line) normal incidence transmission spectra of a TiO_2-SiO_2 double-layered film prepared from a $(PDDA/SiO_2)_6(PDDA/nanosheet)_9$ multilayer assembly. The calculation was based on a 6.5-nm-thick TiO_2/55-nm-thick SiO_2 double-layered structure.

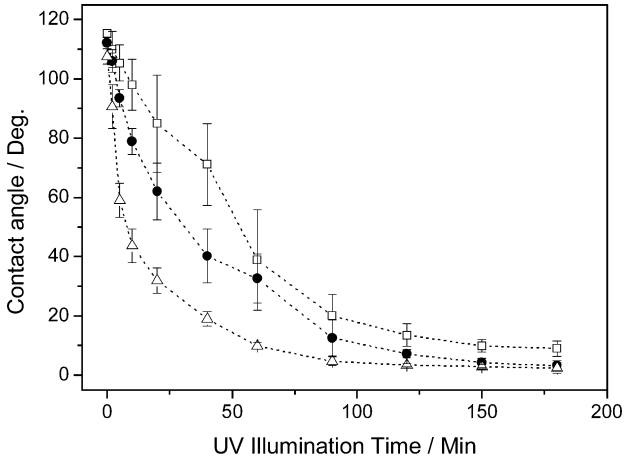

Figure 7. Water contact angle change of ODP-modified TiO_2/SiO_2 double-layer films under UV illumination. The double-layered films were prepared from $(PDDA/SiO_2)_3/(PDDA/nanosheet)_3$ (squares), $(PDDA/SiO_2)_3/(PDDA/nanosheet)_6$ (circles), and $(PDDA/SiO_2)_3/(PDDA/nanosheet)_9$ multilayer assemblies (triangles).

organic substances under UV illumination.[9,10] The oxidation proceeds via photogenerated holes in the valence band of TiO_2, whose redox potential is sufficiently positive to oxidize most types of organic substances.[9,10] The oxidation may also proceed via hydroxyl radicals created by oxidizing water molecules with holes, whose redox potential ($^{\bullet}OH/OH^-$) is only slightly less positive than that for holes and is in fact still more positive than that for ozone (O_3/O_2).[9,10] Superoxide ions, generated by reduction of dioxygen with photogenerated electrons together with molecular dioxygen, also take part in the decomposition of organic substances.[8−11] Thus, TiO_2 can keep its surface free from organic contamination under UV illumination, provided the rate of photocatalytic mineralization is higher than the contamination rate.[8−11] The double-layered TiO_2-SiO_2 film with a 6.5-nm-thick TiO_2 layer was able to decompose almost all of the ODP monolayer under 3 h of UV illumination (2.6 mW cm^{-2}), corresponding to a thinning rate of ~0.8 nm h^{-1} for a hydrocarbon layer. A commercially available self-cleaning glass (Activ, Pilkington), however, decomposed a stearic acid layer at a rate of 1.9 nm h^{-1} under 6.9 mW cm^{-2} UV light, as reported by Mills et al.[15] Considering the different UV intensity, the photocatalytic activity of our double-layered film is quite comparable to the commercial self-cleaning glass. Reflection

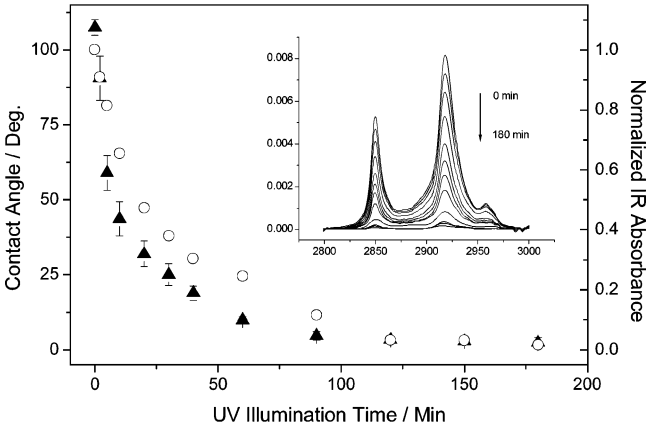

Figure 8. Decay of normalized IR absorbance recorded on a TiO_2-SiO_2 double-layered film covered with an ODP monolayer during UV illumination: vibrations related to the methyl and methylene groups (circles). The double-layered film was prepared from a $(PDDA/SiO_2)_6/(PDDA/nanosheet)_9$ multilayered assembly. For comparison, the decay of the water contact angle (triangles) recorded on the same sample during UV illumination is also shown. Inset: IR spectra of the same sample during UV illumination.

at the surface of the commercial product, however, was approximately 5−7% in the visible spectrum, greater than the 4% reflection of common soda-lime glass.[15]

The double-layered TiO_2-SiO_2 films were all superhydrophilic, with water contact angles smaller than 3° just after preparation, no matter how thick the TiO_2 layer was. Single-layered TiO_2 films prepared by the same layer-by-layer assembly procedures, however, showed a water contact angle of ~5°. The slightly smaller contact angle of double-layered films is possibly due to its rougher surface morphology (Figure 3f). As described by Wenzel et al., the apparent contact angle of a hydrophilic surface will be lowered from its intrinsic contact angle by introducing surface roughness.[45] Storing the double-layered films in the dark over two weeks only caused a slight increase in the water contact angle, but UV illumination soon lowered the contact angle to almost 0°. The superhydrophilic properties of the films were also reflected in Figure 8, where the films showed a nearly 0° water contact angle after complete decomposition of the ODP monolayer. The good superhydrophilic properties allow water to uniformly spread and flow on the films and thus favors the self-cleaning process in outdoor uses.[8−10,15,16]

Conclusions

It has been demonstrated that the dual functions of self-cleaning and antireflection could be created in double-layered TiO_2-SiO_2 nanostructured films. The double-layered film, consisting of a porous bottom SiO_2 layer and a dense top TiO_2 layer, can be readily prepared by layer-by-layer assembly of SiO_2 nanoparticles and titanate nanosheets. The top TiO_2 layer, which has photocatalytic and superhydrophilic properties, is employed to provide the self-cleaning function. The bottom SiO_2 layer, which is of low refractive index, is decisive for creating the antireflective properties. The double-layered film, prepared from a $(PDDA/SiO_2)_6/(PDDA/nanosheet)_9$ multilayer assembly, showed comparable photocatalytic activity to that of Pilkington Activ self-cleaning glass and much better transmittance properties. Further optimization of the film structure, for example, by fine-tuning the thicknesses and porosities of the SiO_2 and TiO_2 layers, may provide improved self-cleaning and antireflective properties.

Acknowledgment. This work was supported by a Grant-in-Aid for Scientific Research on Priority Area 417 from the

Ministry of Education, Culture, Sports, Science and Technology of the Japanese Government and by the Core Research for Evolutional Science and Technology Program of the Japan Science and Technology Agency. The authors thank Dr. H. Uetsuka for providing the titanate nanosheet suspension and Dr. D. A. Tryk for a careful reading of the manuscript and helpful discussion.

Supporting Information Available: X-ray diffraction patterns showing that calcining titanate nanosheet powders at 500 °C caused the phase transition from lamellar structure to anatase structure. This material is available free of charge via the Internet at http://pubs.acs.org.

References and Notes

(1) Fujishima, A.; Honda, K. *Nature* **1972**, *238*, 37.
(2) Hagfeldt, A.; Grätzel, M. *Chem. Rev.* **1995**, *95*, 49.
(3) Grätzel, M. *J. Photochem. Photobiol., C* **2003**, *4*, 145.
(4) Fujishima, A.; Zhang, X.-T. *Proc. Jpn. Acad., Ser. B* **2005**, *81*, 33.
(5) Hoffmann, M. R.; Martin, S. T.; Choi, W.; Bahnemann, D. W. *Chem. Rev.* **1995**, *95*, 69.
(6) Mills, A.; LeHunte, S. *J. Photochem. Photobiol., A* **1997**, *108*, 1.
(7) Stafford, U.; Gray, K. A.; Kamat, P. V. *Chem. Rev.* **1996**, *3*, 77.
(8) Fujishima, A.; Hashimoto, K.; Watanabe, T. *TiO_2 Photocatalysis Fundamentals and Applications*; BKC, Inc.: 1999.
(9) Fujishima, A.; Rao, T. N.; Tryk, D. A. *J. Photochem. Photobiol., C* **2000**, *1*, 1.
(10) Fujishima, A.; Zhang, X. *C. R. Chim.* **2006**, *9*, 750.
(11) Heller, A. *Acc. Chem. Res.* **1995**, *28*, 503.
(12) Paz, Y.; Heller, A. *J. Mater. Res.* **1997**, *12*, 2759.
(13) Paz, Y.; Luo, Z.; Rabenberg, L.; Heller, A. *J. Mater. Res.* **1995**, *10*, 2842.
(14) Minabe, T.; Tryk, D. A.; Sawunyama, P.; Kikuchi, Y.; Hashimoto, K.; Fujishima, A. *J. Photochem. Photobiol., A* **2000**, *137*, 53.
(15) Mills, A.; Lepre, A.; Elliott, N.; Bhopal, S.; Parkin, I. P.; O'Neil, S. A. *J. Photochem. Photobiol., A* **2003**, *160*, 213.
(16) Wang, R.; Hashimoto, K.; Fujishima, A.; Chikuni, M.; Kojima, E.; Kitamura, A.; Shimohigoshi, M.; Watanabe, T. *Nature* **1997**, *388*, 431.
(17) Wang, R.; Hashimoto, K.; Fujishima, A.; Chikuni, M.; Kojima, E.; Kitamura, A.; Shimohigoshi, M.; Watanabe, T. *Adv. Mater.* **1998**, *10*, 135.
(18) Reflection at the TiO_2 surface for the normal incidence can be as high as 19%, as described by the simplified Fresnel equation, $R = (n - 1)^2/(n + 1)^2$, where n is the refractive index of the solid substrate. In contrast, reflection at the glass surface is only approximately 4% for normal incidence due to the lower refractive index of ~1.5.
(19) Ballif, C.; Dicker, J.; Borchert, D.; Hofmann, T. *Sol. Energy Mater. Sol. Cells* **2004**, *82*, 331.
(20) Furbo, S.; Jivan Shah, L. *Sol. Energy* **2003**, *74*, 513.
(21) Yoldas, B. E. *Appl. Opt.* **1980**, *19*, 1425.
(22) Walheim, S.; Schäffer, E.; Mlynek, J.; Steiner, U. *Science* **1999**, *283*, 520.
(23) Hattori, H. *Adv. Mater.* **2001**, *13*, 51.
(24) Hiller, J.; Mendelsohn, J. D.; Rubner, M. F. *Nat. Mater.* **2002**, *1*, 59.
(25) Zhang, X.-T.; Sato, O.; Taguchi, M.; Einaga, Y.; Murakami, T.; Fujishima, A. *Chem. Mater.* **2005**, *17*, 696.
(26) Sasaki, T.; Ebina, Y.; Kitami, Y.; Watanabe, M.; Oikawa, T. *J. Phys. Chem. B* **2001**, *105*, 6116.
(27) Sakai, N.; Ebina, Y.; Takada, K.; Sasaki, T. *J. Am. Chem. Soc.* **2004**, *126*, 5851.
(28) Sasaki, T.; Nakano, S.; Yamauchi, S.; Watanabe, M. *Chem. Mater.* **1997**, *9*, 602.
(29) Sasaki, T.; Ebina, Y.; Fukuda, K.; Tanaka, T.; Harada, M.; Watanabe, M. *Chem. Mater.* **2002**, *14*, 3524.
(30) Wang, L. Z.; Sasaki, T.; Ebina, Y.; Kurashima, K.; Watanabe, M. *Chem. Mater.* **2002**, *14*, 4827.
(31) Lvov, Y.; Ariga, K.; Onda, M.; Ichinose, I.; Kunitake, T. *Langmuir* **1997**, *13*, 6195.
(32) Sennerfors, T.; Bogdanovic, G.; Tiberg, F. *Langmuir* **2002**, *18*, 6410.
(33) Rouse, J. H.; Ferguson, G. S. *J. Am. Chem. Soc.* **2003**, *125*, 15529.
(34) Cebeci, F. C.; Wu, Z.; Zhai, L.; Cohen, R. E.; Rubner, M. F. *Langmuir* **2006**, *22*, 2856.
(35) Sasaki, T.; Ebina, Y.; Tanaka, T.; Harada, M.; Watanabe, M. *Chem. Mater.* **2001**, *13*, 4661.
(36) Sakai, N.; Fukuda, K.; Shibata, T.; Ebina, Y.; Takada, K.; Sasaki, T. *J. Phys. Chem. B* **2006**, *110*, 6198.
(37) Sasaki, T.; Watanabe, M.; Hashizume, H.; Yamada, H.; Nakazawa, H. *J. Am. Chem. Soc.* **1996**, *118*, 8329.
(38) Sasaki, T.; Watanabe, M. *J. Am. Chem. Soc.* **1998**, *120*, 4682.
(39) Textor, M.; Ruiz, L.; Hofer, R.; Rossi, A.; Feldman, K.; Hahner, G.; Spencer, N. D. *Langmuir* **2000**, *16*, 3257−3271.
(40) The thickness of the ultrathin TiO_2 layer was estimated by ellipsometry on the samples prepared on quartz substrates directly, without the SiO_2 porous interlayer.
(41) Yoffe, A. D. *Adv. Phys.* **1993**, *42*, 137.
(42) Macleod, H. A. *Thin Film Optical Filters*; Hilger: Bristol, U. K., 1986.
(43) The thickness of the porous SiO_2 layer prepared by heating the $(PDDA/SiO_2)_6$ multilayer film was estimated to be 55 nm by ellipsometry. This thickness was smaller than the ca. 65 nm thickness estimated by cross-sectional electron micrographs.
(44) Folkers, J. P.; Gorman, C. B.; Laibinis, P. E.; Buchholz, S.; Whitesides, G. M.; Nuzzo, R. G. *Langmuir* **1995**, *11*, 813.
(45) Wenzel, R. N. *Ind. Eng. Chem.* **1936**, *28*, 988.